water

MDPI

Article

Assessing the TSS Removal Efficiency of Decentralized Stormwater Treatment Systems by Long-Term In-Situ Monitoring

Christian Lieske *, Dominik Leutnant and Mathias Uhl

Institute for Water Resources Environment (IWARU), Muenster University of Applied Sciences, Corrensstraße 25, 48149 Muenster, Germany; Leutnant.Dominik@eglv.de (D.L.); uhl@fh-muenster.de (M.U.)
* Correspondence: christian.lieske@fh-muenster.de; Tel.: +49-251-8365299

Abstract: Decentralized treatment of stormwater runoff from heavily polluted surface can be a good solution for effective source control. Decentralized stormwater treatment systems (DS) and test procedures to monitor their performance, have been developed in recent years. At present in Germany, only lab-based tests are officially established to determine the removal efficiency of Total Suspended Solids (TSS), and in situ monitoring is still lacking. Furthermore, the fine fraction of TSS with particle sizes less than 63 µm (TSS63) have been established as a new design parameter in Germany, because of their substitute characteristics of adsorbing pollutant substances. For research and evaluation purposes continuous data of urban stormwater runoff quantity and quality at the in- and outflow of two different DS at two different sites were collected. Turbidity is used as a surrogate for TSS. Continuous turbidity data and time proportional sampling served to obtain (i) regression coefficients and (ii) to determine the TSS removal efficiency of DS. For a wide range of events the total removal efficiency of DS1 was 29% for TSS and 19% for TSS63 and for DS2 19% for TSS and 16% for TSS63. An event-based data analysis revealed a high variability of the efficiencies and its uncertainties. Moreover, outwash of still suspended or remobilization of already deposited material was observed at individual events. At both sites TSS63 dominates urban stormwater runoff as indicated by the mean ratios of TSS63 to TSS of 0.78 at the inflows and 0.89 at the outflows of both DS. A significant shift of TSS63 ratio from inflow to outflow demonstrates that TSS63 particles were removed less efficiently than coarser particles by DS1, for DS2 data was too heterogeny. It clarifies that common sedimentation methods can only contribute to a small extent to the reduction of solid emissions if the stormwater runoff contains mainly fine-particle solids. The findings suggest that treatment of urban stormwater runoff with high TSS63 pollution requires additional techniques such as a proper filtering to retain fine particles more effective.

Keywords: urban stormwater runoff quality; decentralized treatment; total suspended solids; continuous monitoring; turbidity measurement

check for updates

Citation: Lieske, C.; Leutnant, D.; Uhl, M. Assessing the TSS Removal Efficiency of Decentralized Stormwater Treatment Systems by Long-Term In-Situ Monitoring. *Water* **2021**, *13*, 908. https://doi.org/10.3390/w13070908

Academic Editor: Brigitte Helmreich

Received: 16 February 2021
Accepted: 24 March 2021
Published: 26 March 2021

1. Introduction

The water quality, ecology, and microbiology of receiving rivers are influenced by separate and combined sewer outlets, in addition to direct street runoff (e.g., [1–3]). Urban runoff transports high loads of particles that also act as main vector for particle-bound pollutants [4–6]. High concentrations and annual loads of heavy metals (Zn > Cu > Pb) have been detected in urban storm water which originated from vehicle brake emissions, tire wear, roof covering materials or atmospheric deposition [4,5,7–10]. With decreasing particle size, the loads of heavy metals rise [11] and correlate significant to fine fraction of Total Suspended Solids (TSS63, with particles sizes of 0.45 µm < TSS63 < 63 µm) [12]. The characteristic of fine particles as TSS63 is classified by Hilliges (2017) according to ISO 14688 as a divide between settleable and non-settleable particles. Based on studies of Hilliges et al. (2017), Dierschke and Welker (2015), Zhao et al. (2010) and Selbig (2015) that

focus on distribution and pollution of particles in road runoff, TSS63 was implemented in 2020 as a new design parameter in German stormwater management regulation [12–16].

Conventional sewer systems convey the stormwater runoff from different polluted areas to central treatment facilities, such as stormwater treatment tanks. As runoff of different areas with different levels of pollution becomes concertedly treated, even runoff from areas with low pollution must be treated. Additionally, highly polluted runoff gets diluted by low polluted runoff, meaning that the treatment system requires a higher hydraulic capacity and retention. As a consequence, the less polluted stormwater is missing in the catchment area for infiltration and evaporation, which interrupts the natural water cycle. Furthermore, hydraulic pressure and less pollution load can reduce the efficiency of treatment. Therefore, decentralized stormwater treatment systems that ensure treatment close to pollution sources provide a chance to efficiently reduce stormwater related emissions to the receiving water.

In recent decades, various decentralized stormwater treatment systems have been developed (e.g., [17,18]). These systems vary in shape and size, from road gullies, swales, manholes, and multiple chamber tanks, to sewer conduits of up to 12 m length (e.g., [17]). They often aim to combine treatment mechanisms, such as hydraulic retention, sieving, sedimentation, light fluid separation, filtration, and retention of dissolved heavy metals (e.g., [17]).

To ensure a quality control of their performance, various testing and approval procedures have been internationally developed that require standardized laboratories or several representative events under in situ conditions [18–22]. The determination of in situ pollutant removal is conducted with automatic sampling and based on flow proportional sampling [18–20]. However, little is known about the in situ efficiencies of these systems under long-term operation, especially for the new design parameter TSS63. Furthermore, the removal efficiency of sedimentation technologies in DS is of fundamental importance in view of the dominant fine particles and associated pollutants in stormwater runoff and their importance for catchment-wide stormwater management strategies [12].

Much progress has been made in the continuous monitoring of stormwater runoff quality using UV-vis-spectrometers or turbidity sensors to study intra-event pollutant dynamics and to estimate event pollutant loads [23–29]. These studies showed site- and event-specific characteristics of the occurrence and composition of pollutants, and revealed the highly stochastic nature of the build on and wash off processes, which may influence the removal efficiencies of DS as well.

The present study therefore intends to contribute findings regarding the following key questions:

(i) Is turbidity a sufficiently useful surrogate parameter for concentration and composition in the influent and effluent of DS?
(ii) How high are the TSS and TSS63 removal efficiencies during in situ long-term operation and how do they vary?
(iii) What are the deterministic and stochastic components of the efficiencies?

For this purpose, experimental investigations of two different DS at two different locations were carried out, and the results thereof are reported here.

2. Materials and Methods

2.1. Monitoring Sites

Measurements were conducted at two sites, both located in the city of Münster, Germany (see Table 1 and Figure 1 for details). The catchment "Stadtgraben" (SG) (2.63 ha, DS coordinates 51°57′32.152″ N, 7°37′8.253″ E(WGS84)) is located close to the city center and dominated by a high traffic road and surrounded by commercial and office buildings. Stormwater runoff is collected by a separate sewer with a diameter of 500 mm and 6‰ to 7‰ slope. The catchment "Canisiusgraben" (CG) (10.47 ha, DS coordinates 51°56′28.447″ N, 7°35′43.407″ E (WGS84)) is a residential area with flat and steep roofs and

two main roads as major pollution sources. The storm sewer system ends with a diameter of 800 mm and 2.5‰ slope.

Table 1. Catchment characteristics of monitoring sites.

Site	Total Size	Impervious Area				Slope	Traffic Load
		Sum (Cover)	Roofs	Sidewalks	Streets		
-	ha	ha (%)	ha	ha	ha	‰	Vehicles per day
Stadtgraben (SG)	2.63	2.5, (95)	0.63	0.27	1.6	5.5	30,000
Canisiusgraben (CG)	10.7	5.7, (53)	2.51	0.83	2.36	10 to 13	9000 and 13,000

Figure 1. Location of monitoring sites in Münster (**B**) and in detail: Canisiusgraben (**A**) and Stadtgraben (**C**), with decentralized stormwater treatment systems (DS) positions (green marks), rain gauge (RG) positions (blue infopoint marks), and sewer catchment (orange and red framed areas). (Image © 2021 Google Earth).

2.2. Decentralized Stormwater Treatment Systems

DS1 at site SG is a SediPipe XL 600/12 (Fränkische Rohrwerke Gebr. Kirchner GmbH & Co. KG; Königsberg, Germany) that was installed in 2017. The pipe with 600 mm diameter and 12 m length operates as a permanently filled sedimentation unit with counter gradient. A special grate near the bottom prevents detachment of already settled sediments. An immersion tube in front of the outlet retains floating materials and light liquids (cf. schematic in Appendix A, Figure A1). In case of an event, stormwater is constantly pumped into DS1 at the rate of 6 L/s by a peristaltic pump (P-50-classic twin, Ponndorf, Kassel, Germany,). This corresponds to the runoff maximum of 0.4 ha impervious area recommended by the manufacturer.

DS2 was installed in 2018 at site CG and is a ViaTub 18R63 Lamella Clarifier (Mall GmbH, Donaueschingen, Germany,). The circular concrete tank with a diameter of 3 m contains a lamella separator for enhanced sedimentation in surcharged conditions (cf. schematic in Appendix A, Figure A2). The inflow from the storm sewer is limited to 35 L/s by a flow-controlled throttle valve. The lamella clarifier is operated according to valid regulations and is equipped with a side weir for discharges above the critical discharge level.

2.3. Measurement Equipment

The continuous stormwater quality measurements at the in- and outlet of a DS comprise turbidity, electrical conductivity, and pH (with sensors VisoTurb 700 IQ, TetraCon 700 IQ and SensoLyt 700 IQ, respectively all Xylem Analytics Germany Sales GmbH & Co. KG, WTW, Weilheim in Oberbayern, Germany). Turbidity value is used as a surrogate for TSS. Electrical conductivity (EC) is measured to validate the start of an event, monitor the use of deicing salts during the cold season, and support analysis of heavy metals at DS due to the fact that higher EC correlates significantly with an increase in total Zn [12]. The pH value is targeted as a supporting parameter for the interpretation of dissolved heavy metals. In particular, at DS with backwater, the pH value can change during longer dry periods due to redissolution of particle bound pollutants in anaerobic areas [30]. Measurement of the primary parameter turbidity is based on 90° scattered light measurement according to DIN EN ISO 7027 [31] and is expressed in Formazine-Nephelometric Units (FNU) equal to a Nephelometric Turbidity Unit (NTU). The turbidity-sensor measurement range is from 0 to 4000 FNU, and resolution ranges between 0.001 FNU to 1 FNU and depends on the current measured value. Process variation coefficient is less than 1% in the range up to 2000 FNU according to DIN 38402-51 [31]. In- and outlet sensors are connected to a central transmitter (MIQ/TX 2020 XT, WTW, Weilheim, Germany) with data values logged in 1-min time steps.

Sewer water level sensors (OCL-L1/DSM, NIVUS; Eppingen, Germany) with uncertainty u $\leq \pm 0.5\%$ of final value or ± 5 mm [32] and combined sensors for flow velocity and water level (POA-V2H1/V2U1/CSM-D, NIVUS, Eppingen, Germany,) with velocity u = $\pm 0.5\%$ to 1% of final value and pressure u $\leq 0.5\%$ of final value [32], are installed on sites. The water level value is used to trigger automatic sampling (ASP station, Endress + Hauser, Rheinach, Switzerland,) and the start of pumping at site SG. At the site SG the rain gauge (Pluvio2, OTT Hydromet, Kempten, Germany,) is installed on a flat roof (cf. Figure 1C, RG Paulinum) and collects data with a 0.01 mm threshold [33], logged in 1-min time steps. Precipitation data are recorded with the same system and configuration on a flat roof of one of the university buildings (cf. Figure 1B, RG FHZ) and used for site CG.

2.4. Sampling Method and TSS Analysis

The water level value (threshold criteria: 3 cm at SG and 5 cm at CG, each with 0.5 cm hysteresis) started and ended automatic time continuous sampling. The sampling procedure consisted of 200 mL sample shots every 2 min and a merging of 5 shots into one composite sample of 1 L for a maximum of 12 polyethylen (PE) bottles per event (for rain event statistics see Appendix A Table A1). Sample storage sections on site and in laboratory were constantly cooled to 4 °C. In the laboratory, each composite sample was analyzed for turbidity (VisoTurb 700 IQ) and TSS according to DIN 38409-2 1987 [34] comparable to the Environmental Protection Agency (EPA) Method 160.2 [35] and Standard Method 2540D [36] with a 0.45 µm cellulose nitrate membrane filter (Typ11306, Sartorius, Goettingen). For turbidity measurement, a black cylindrical polyethylene high density (PE-HD) bottle was used, and the sample was homogenized with a magnet stirrer at 450 rpm as described in [23]. TSS was divided into the two compartments TSScoarse (2 mm > x > 63 µm) and TSS63 (63 µm > x > 0.45 µm) by sieving (2 mm and 63 µm test sieve, Retsch GmbH, Haan, FRG). Because a standard operating procedure for separation and analysis of TSS63 [37] was missing, the method recommended by [14] was applied.

2.5. Data Processing and Management

For data import, backup, and analysis OSCAR, a data management system developed by one of the authors, was used [38]. Measurement data per site and sensor were stored using an open-source time series platform (InfluxData, San Francisco, 2020 [39]) and visualized with a web interface (Grafana Labs, New York, 2020 [40]).

For both sites, the following data processing and analysis were conducted with reference to [41]: (i) verification, (ii) correction, (iii) transformation (linear regression turbidity

to TSS), (iv) event selection and (v) calculation of event parameters. Event statistics (description, duration, intensities) were calculated for rainfall, runoff and loads. The event selection criteria were minimum rainfall depth H > 2 mm and maximum rainfall intensity in 60 min Imax60 > 2 mm/h, and additionally at site CG, bypass volume < 1 m^3 per event.

TSS composite samples were checked for distribution and their effect on the goodness of fit of linear turbidity to TSS regression. In particular, the TSS63 ratio was considered and evaluated regarding the effect on regression coefficients. Further values with relative residuals > 3 σ and diagnosed using the function influence measures in R [42] were determined as outliers.

2.6. Determination of Load Removal Efficiencies

To determine the event-specific and site-specific TSS load B_E (kg), continuous turbidity measurements were converted into TSS concentration c_{TSS} (mg/L) with a linear regression model, using Equation (1) according to [27,43,44]. B_E for in- and outflow was obtained from the product of $c_{TSS,i}$ and discharge Q_i (m^3/s), and multiplied with the measuring interval Δt (i.e., 1 min) according to Equation (2). The TSS removal efficiency $\eta_{E,B}$ is determined with Equation (3).

$$\text{TSS concentration (mg/L)}: c_{TSS}\left(\frac{mg}{L}\right) = f(turbidity) = a + b \times turbidity \quad (1)$$

where a = intercept, b = slope

$$\text{TSS event load (kg)}: B_E = \sum_{i=1}^{n}(Q_i c_{TSS,i}\,\Delta t_i) \quad (2)$$

where i = index of the time series, n = number of time steps of an event

$$\text{TSS removal efficiency (\%)}: \eta_{E,B} = 1 - \frac{B_{E,out}}{B_{E,in}} \times 100 \quad (3)$$

where $B_{E,out}$= event TSS load in the outflow, $B_{E,in}$ = event TSS load in the inflow.

TSS63 concentration c_{TSS63} (mg/L) as a fraction of TSS cannot be derived directly from turbidity data. Therefore, as a first approximation to estimate a TSS63 removal efficiency $\eta_{E,B,TSS63}$ (%), the mean value of the gravimetrically determined ratio of TSS63 to TSS from composite samples was considered. The ratio f (-) of c_{TSS63} and c_{TSS} was obtained with Equation (4). The $\eta_{E,B,TSS63}$ was calculated with Equation (5). For the opposite fraction of TSS63, a first estimation of its removal efficiency $\eta_{E,B,TSScoarse}$ (%) was calculated using Equation (6).

$$\text{Ratio of TSS63 and TSS } (-): f = \frac{c_{TSS63}}{c_{TSS}} \quad (4)$$

$$\text{TSS63 removal efficiency estimation (\%)}: \eta_{E,B,TSS63} = 1 - \frac{B_{E,out} f_{out,mean}}{B_{E,in} f_{in,mean}} \times 100 \quad (5)$$

with $f_{out,mean}$ = mean ratio of TSS63 to TSS in the outflow, $f_{in,mean}$ = mean ratio of TSS63 to TSS in the inflow

$$\text{TSScoarse removal efficiency estimation (\%)}: \eta_{E,B,TSScoarse} = 1 - \frac{B_{E,out}(1 - f_{out,mean})}{B_{E,in}(1 - f_{in,mean})} \times 100 \quad (6)$$

2.7. Determination of Uncertainties

Two key values are subject to uncertainty estimations according to ISO/IEC Guide 98-3:2008 [45]. Of major interest are (i) the uncertainty of the ratio f of TSS63 and TSS

resulting from lab analysis and (ii) the uncertainty of the removal efficiency η_E caused by turbidity measurements as a proxy for TSS.

$$\text{Uncertainty of TSS63 ratio } (-)\text{: } u_f = \sqrt{\left(\frac{1}{c_{TSS}^2}\right) \times u_{c,TSS63}^2 + \left(\frac{c_{TSS63}^2}{c_{TSS}^4}\right) \times u_{c,\,TSS}^2} \quad (7)$$

$$\text{Relative uncertainty of TSS63 ratio } (-)\text{: } u_f^* = \frac{u_f}{f} \quad (8)$$

The ratio f of c_{TSS63} and c_{TSS} and its uncertainty u_f and relative uncertainty u_f^* are expressed with Equations (4), (7) and (8).

The uncertainty of the concentrations $u_{c,TSS}$ (-) and $u_{c,TSS63}$ (-) were estimated using the Type B method [45]. From previous analytical quality assurance, it can be assumed that the lab results for c_{TSS63} and c_{TSS} are normally distributed with a 95%-confidence interval of ± 10%. The relative standard uncertainty according to [45] is therefore $u_{c,TSS}^* = u_{c,TSS63}^*$ = 0.03876.

To study the single uncertainty effect of turbidity measurement as proxy for c_{TSS} the discharge uncertainty u_Q and time series covariance were set to zero. For each time interval t_i (min) the mass flow rate $\dot{m}_i$(kg/s) and its uncertainty $u_{m,i}$ (-) were calculated by Equation's (9), (10) and (11). The calculation of uncertainty of the event-specific TSS load $u_{B,E}$ is expressed by Equation (12).

$$\text{Mass flow rate (kg/s)}\text{: } \dot{m}_i = Q_i \times c_{TSS,i} \quad (9)$$

$$\text{Uncertainty of mass flow rate } (-)\text{: } u_{\dot{m},i} = \sqrt{Q_i^2 \times u_{c,TSS,i}^2 + c_{TSS,i}^2 \times u_{Q,i}^2} \quad (10)$$

$$= \sqrt{Q_i^2 \times u_{c,TSS,i}^2} \quad (11)$$

where i = index of the time series, Q_i = discharge at time i.

$$\text{Uncertainty of event load } (-)\text{: } u_{B,E} = \Delta t \times \sqrt{\sum_{i=1}^{n} u_{m,i}^2} \quad (12)$$

where i = index of the time series, n = number of time steps of an event, and Δt = measuring interval

The removal efficiency $\eta_{E,B}$ and its uncertainty $u_{\eta_{E,B}}$ and relative uncertainty $u_{\eta_{E,B}}^*$ can be calculated from the TSS loads of the DS inflow $B_{E,in}$ and outflow $B_{E,out}$ and their uncertainties $u_{B,E,in}$ and $u_{B,E,out}$t, respectively, by Equations (13) and (14).

$$\text{Uncertainty of removal efficiency } (-)\text{: } u_{\eta_{E,B}} = \sqrt{0^2 + \left(\left(\frac{1}{B_{E,in}^2}\right) \times u_{B,E,out}^2 + \left(\frac{B_{E,in}^2}{B_{E,out}^4}\right) \times u_{B,E,in}^2\right)} \quad (13)$$

$$\text{Relative uncertainty of removal efficiency } (-)\text{: } u_{\eta_{E,B}}^* = \frac{u_{\eta_{E,B},}}{\eta_{E,B}} \quad (14)$$

The concentrations were calculated using a regression model with Equation (1). The uncertainty of the regression model is increased by the uncertainties of turbidity measurement and TSS analysis. Therefore, the residuals Δc (mg/L) between the model-based concentrations c_{calc} (mg/L) and the lab analysis c_{lab} (mg/L) therefore result from multiple sources and can be used to estimate the uncertainties of the concentration c. The residuals Δc and the relative residuals Δc^* can be obtained with Equations (15) and (16).

$$\text{Residuals (mg/L)}\text{: } \Delta c = c_{calc} - c_{lab} \quad (15)$$

$$\text{Relative Residuals } (-)\text{: } \Delta c^* = \frac{\Delta c}{c_{calc}} \quad (16)$$

The relative uncertainty u_c^* can be estimated using the Type A method [45] from the standard deviation $s_{\Delta c^*}$ of the relative residuals Δc^* of $i = n$ data pairs ($c_{calc,i}$; $c_{lab,i}$) by $u_c^* = s_{\Delta c^*}$. The uncertainty $u_{c,i}$ of the concentration time series data can be estimated by:

$$\text{Uncertainty of concentration } (-)\text{: } u_{c,i} = c_{calc,i} \times u_c^* \tag{17}$$

It is important to note that the above-mentioned procedure only aims to identify the influence of uncertainties of turbidity as a proxy for TSS concentration data. It therefore sets uncertainties of discharge and covariances to zero. Both must be considered for total uncertainty calculations.

3. Results

Presentation of the results follows the process of sample evaluation, starting with the analysis of composite samples. Next, the regression model is shown that is based on TSS analysis. With the determined coefficients the turbidity data are converted to TSS for calculation of loads and removal efficiencies. The calculation is followed by a further examination of the uncertainties. In the last step a mass balance is determined based on composite samples.

3.1. Analysis of TSS and TSS63

Sampling was carried out from January 2018 to July 2019. To derive the regression function at the site "Stadtgraben" (SG) 210 inflow and 91 outflow composite samples of 1 L were analyzed. At the site "Canisiusgraben" (CG) 221 samples were taken from the inflow and 189 from the outflow. Table 2 lists the descriptive statistics of the evaluated TSS concentrations for 2018 (all seasons), for 2019 (without fall and winter) and a summary of all samples (rain statistics are shown in Appendix A Table A1, TSS statistics are shown in Appendix A Table A2). At site SG, a previous catchment study recorded TSS concentrations in sewers with median TSS concentration in 2015 (67.1 mg/L) between observed values of 2018 (123 mg/L) and 2019 (32.1 mg/L) [23]. The previous study did not cover TSS63 concentrations.

Table 2. Descriptive statistics of TSS concentration and TSS63 ratio from composite samples per site, sample position, and year with raw data. SG data are compared to previous sewer data from [23].

Site	Sample Position	Year	n	c_{TSS} Mean	c_{TSS} sd	c_{TSS} Median	$f\frac{c_{TSS63}}{c_{TSS}}$ Mean	$f\frac{c_{TSS}}{c_{TSS63}}$ sd
-	-	-	-	mg/L	mg/L	mg/L	-	-
SG	Sewer	2015	85	63.7	31.7	67.1	-	-
	Inflow	2018	107	172	184	123	0.80	-
		2019	103	80.4	135	32.1	0.76	-
		all	210	127	168	81.2	**0.78**	0.19
	Outflow	2018	67	127	88.4	110	0.91	-
		2019	24	36.1	25.2	29.5	0.84	-
		all	91	103	86.8	69.2	**0.89**	0.17
CG	Inflow	2018	128	47.4	60.4	29.2	0.83	-
		2019	93	26.1	24.6	18.2	0.73	-
		all	221	38.4	49.7	25.4	**0.79**	0.19
	Outflow	2018	103	56.1	81.9	29.2	0.86	-
		2019	86	34.0	79.6	10.0	0.78	-
		all	189	46.0	81.4	21.2	**0.82**	0.19

At all sites and sample positions, concentration statistics in 2018 were above the values in 2019. Median values decreased from inflow to outflow at both sites. The overall mean ratios of TSS63 to TSS concentration at SG and CG in the in- and outflow were 0.78, 0.89, 0.79 and 0.82, respectively. Ratios of TSS63 to TSS increased per site from inflow to outflow

by 0.11 at SG and 0.03 at CG. A single factor analysis of variance (ANOVA, with alpha = 0.05) was conducted for TSS63 ratio data samples for in- and outflows per site. The resulting p-value of 5.12 $\times 10^{-6}$ at SG indicates that the TSS63 ratios differed significantly. The result for CG with a p-value of 6.2 $\times 10^{-3}$, indicates no significant shift.

Figure 2 shows the distribution function of determined TSS concentrations. The lower graphs of SG inflow and outflow illustrate the higher TSS pollution of the catchment, in comparison to CG. The progressions of in- and outflow graphs per site are narrow. This is covered by the descriptive TSS statistic.

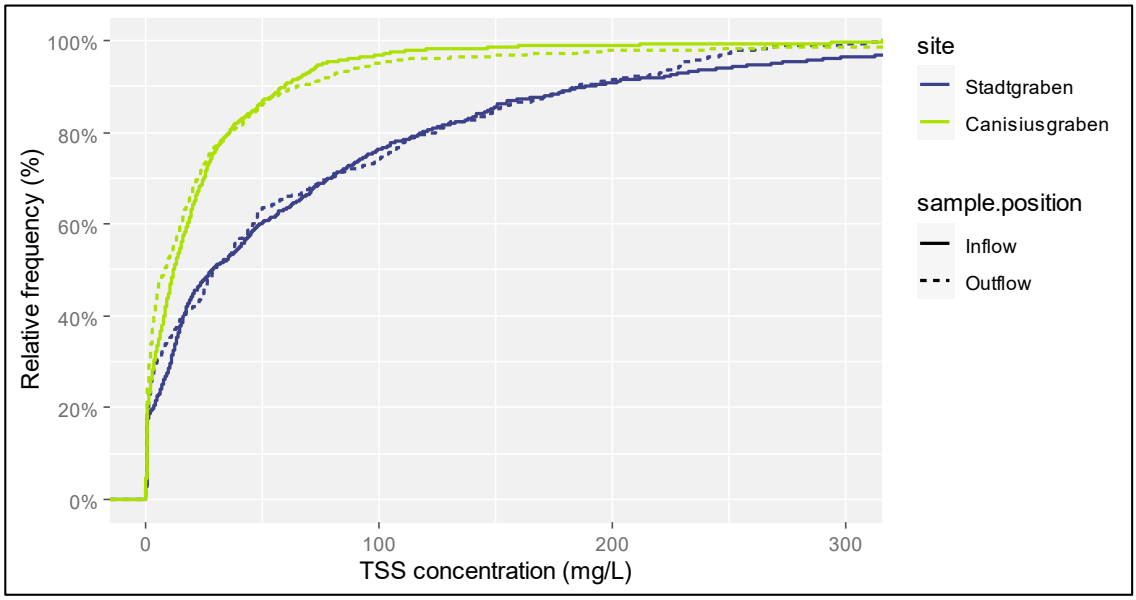

Figure 2. Empirical distribution function of TSS concentration differentiated by site and sample position. TSS concentration data are limited to 300 mg/L of max value of 1300 mg/L to highlight the differences in the dominant data range (cf. Appendix A Table A1).

The TSS63 ratio shift between sample positions and over sampling time is illustrated in Figure 3. Only events with more than six of 12 composite samples were considered (with inflow n = 20 events and outflow n = 8 events, total samples n = 281). Not enough samples were present for the first composite sample at the outflow due to a water level deficit at the beginning of the event. During sampling, the TSS63 ratio at the inflow rose. The increase in TSS63 ratio between inflow and outflow samples is likely to occur due to better removal of coarse particles.

3.2. Relation between TSS and Turbidity

The correlation between turbidity and TSS concentration was determined using linear regression. Table 3 lists the regression coefficients and goodness-of-fit obtained for each site and sample position. In experiments with variable concentration and particle size distribution of quartz flour, the influence of particle size distribution on the resulting turbidity was clarified [43]. It could be shown that samples at constant concentration, but with increasingly higher fine content, cause higher turbidity. For a conversion from TSS data into turbidity this results in a higher slope, whereas a conversion from turbidity data into TSS results in a lower slope as higher the TSS63 ratio is.

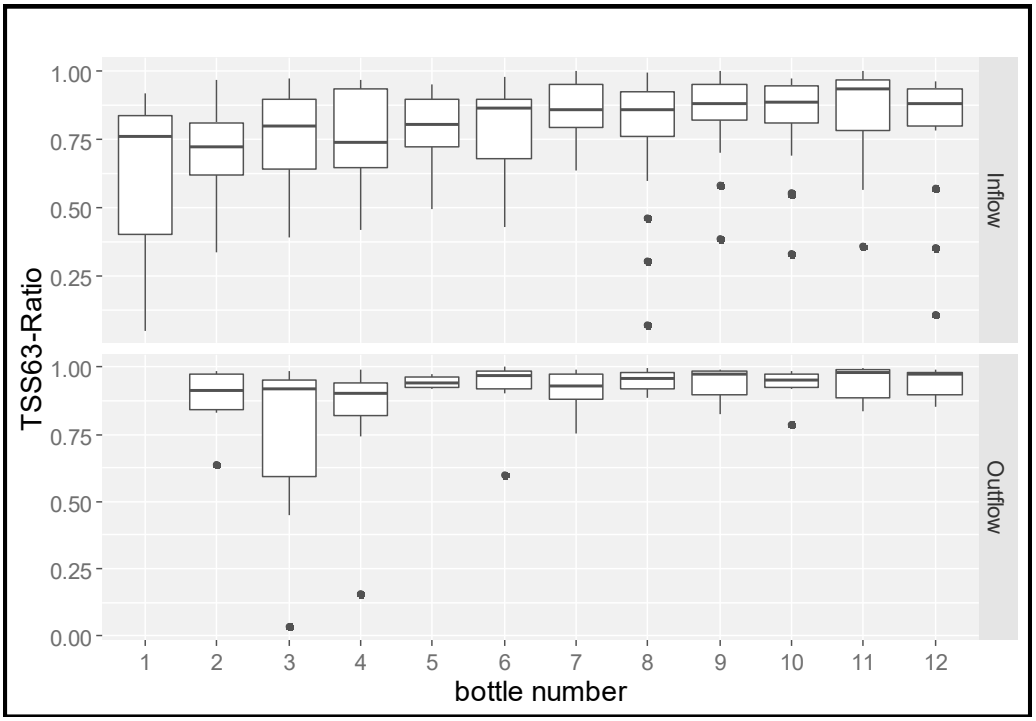

Figure 3. TSS63 ratio per composite sample bottle at SG during event sampling. Each bottle represents a 10 min time step. With numbers of samples per boxplot: for inflow min = 14, and max = 19 and for outflow min = 6, and max = 8. Boxplots with whiskers for inflow and outflow ratios summarize the statistical description of all bottle samples and show mean, median, 0.25 and 0.75 percentile, and 1.5 × inter-quartile range (IQR). Outliers are indicated as black dots.

Table 3. Regression coefficients of TSS and turbidity with corresponding goodness-of-fit, as a comparison of raw and adjusted data.

Site	Sample Position	n	R^2 (Adjusted)	Intercept (a)	Slope (b)	st.error
Stadtgraben	inflow	210 [1]	0.44	−3.84	1.21	0.09
	outflow	91 [1]	0.75	−2.68	0.96	0.06
Canisiusgraben	inflow	221 [1]	0.65	−0.78	0.84	0.04
	outflow	189 [1]	0.44	3.25	0.94	0.08
Stadtgraben	inflow	182 [2]	0.75	2.31	0.99	0.04
	outflow	83 [2]	0.75	−0.41	0.95	0.06
Canisiusgraben	inflow	181 [2]	0.86	−1.94	0.91	0.03
	outflow	166 [2]	0.92	−3.96	0.99	0.02

[1] = raw data samples, [2] = adjusted data samples.

At sites, the average mean TSS63/TSS ratio was close to 0.8 with sd ~ 0.2. To dampen the influence of potential outliers we set mean ± 1.5 × sd as the selection criterion with a resulting TSS63 ratio range for regression of 0.5 to 1.0. This ensures that the final correlation represents most events reliably. Because of the neglect of lower TSS63 ratio samples, the slope coefficient may decrease, which was only recorded for the coefficients of site SG.

After data preparation, the coefficients of R^2 (adjusted) were above 0.75 at the site "Stadtgraben" and above 0.86 at the site "Canisiusgraben". The standard error for slope has decreased, whereas R^2 (adjusted) improved. For site SG, sewer turbidity and TSS concentrations data from a previous study of the catchment [23] are available, with b = 0.97, a = 7.93 and R^2 = 0.68 based on 85 samples from 16 events.

Figure 4 shows the linear relationship between TSS and turbidity that can be observed (A) with and (B) without samples that meet the selection criterion. The similar gradient

coefficients also emphasize a similar particle characteristic per site. Both DS treat the polluted runoff mainly through sedimentation.

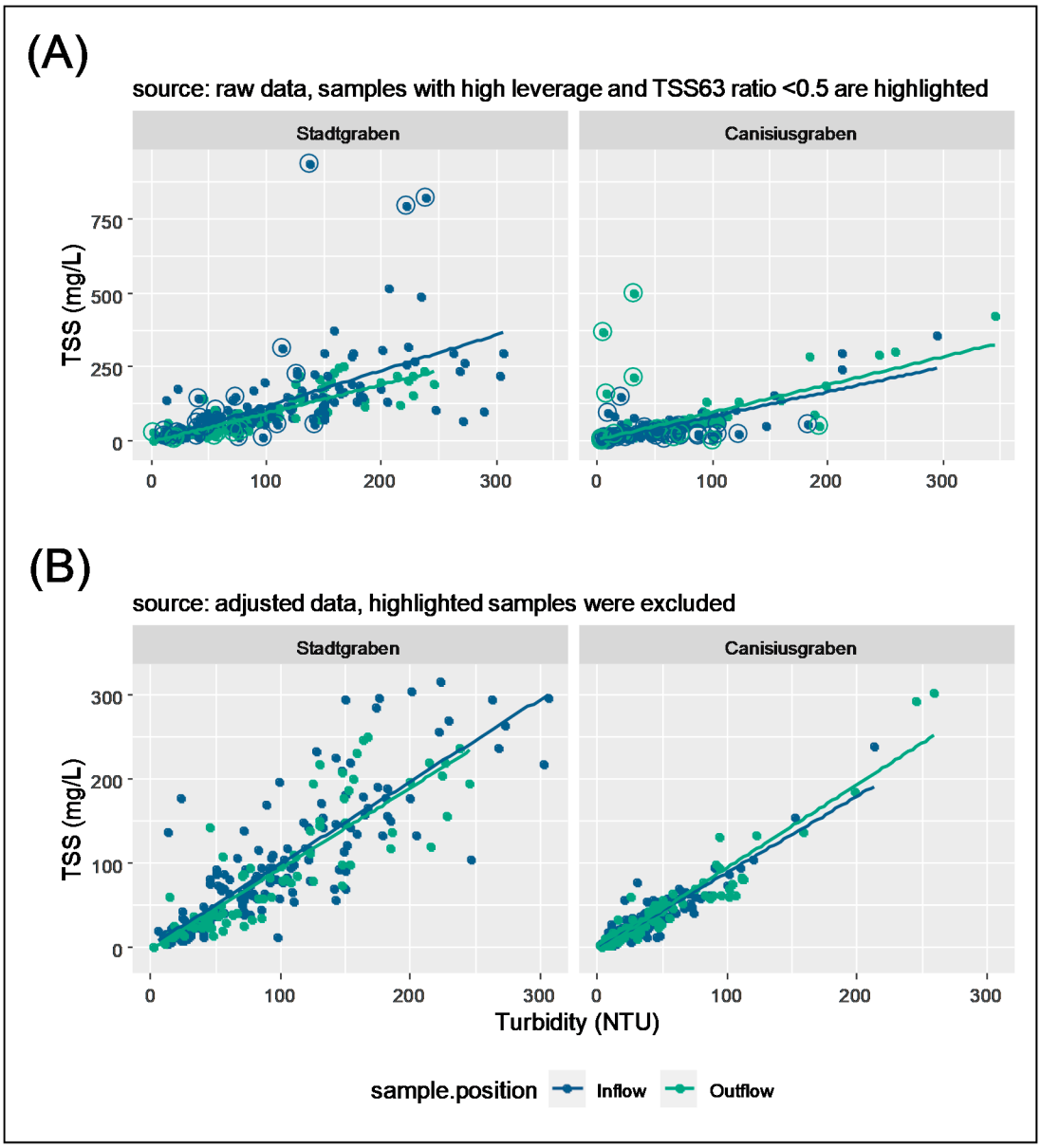

Figure 4. Linear regression of turbidity and TSS before (**A**) and after data preparation (**B**). Dots with circles in (**A**) highlight samples with a high leverage and a TSS63 ratio < 0.5.

3.3. TSS Load Removal Efficencies

The long-term in situ performance of the two DS was evaluated based on continuous turbidity time series. Table 4 lists the determined TSS loads and removal efficiencies of both sites for two periods. Period 1 was the first monitoring cycle that started on November 2017 for SG, on May 2018 for CG and continued until July 2019. In period 1, 2018 with a low rain total was covered. Period 2 covers the prolonged monitoring time until November 2020. The $B_{E,in,median}$ was 7.9 kg (n = 51) and 7.6 kg (n = 91) at site SG and was comparable over both periods. At site CG, $B_{E,in,median}$ decreased in period 2 probably because of fewer valid events with high pollution due to sensor failure.

Table 4. TSS loads and removal efficiency over two monitoring periods for both DS.

Site	Period	Events	TSS Load Inflow Median	TSS Load Inflow Total	TSS Load Outflow Median	TSS Load Outflow Total	TSS Removal Efficiency
	From–to	n	$B_{E,in,median}$	$B_{in}=\sum_{i=1}^{n} B_{E,in,i}$	$B_{E,out,median}$	$B_{out}=\sum_{i=1}^{n} B_{E.,out,i}$	$\eta_B=1-\frac{B_{in}}{B_{out}}\times 100$
		-	kg	kg	kg	kg	%
SG	November 2017–July 2019	51	7.9	812	4.4	485	40
	November 2017–November 2020	91	7.6	1413	5.16	1006	29
CG	May 2018–July 2019	26 [1]	10.3	442	11.7	357	19
	May 2018–November 2020	42 [1]	8.3	556	8.4	452	19

[1] In monitoring period 1, 33 events were valid, and in period 2, 51 events were valid, of which 7 and 9 events, respectively, showed inflows above the critical rainfall bypass discharge volume of >1 m^3. These events were excluded to determine the correct load efficiencies for DS2.

At site SG, the sum of inflow load of the 91 events was B_{in} = 1413 kg, and 407 kg was retained by sedimentation in the DS. This corresponds to a removal efficiency of $\eta_{B,SG}$ = 29% (40% in period 1). For site CG, loads of period 2 were calculated as B_{in} = 556 kg and B_{out} = 452 kg. The removal efficiency of 42 events in period 2 was $\eta_{B,CG}$ = 19%, as before in period 1.

Long-term removal efficiency estimations for TSScoarse (2 mm > x > 63 µm) and TSS63 are given in Table 5. For TSScoarse, the estimated removal efficiencies were $\eta_{B,coarse,SG}$ = 59% and $\eta_{B,coarse,CG}$ = 28%. For TSS63, the estimated removal efficiencies were lower, with $\eta_{B,63,SG}$ = 19% and $\eta_{B,63,CG}$ = 16%.

Table 5. Estimated long-term load and removal efficiencies for TSS fractions TSScoarse and TSS63 at sites SG and CG.

Site	Sample Position	TSS Total Load	TSS Ratio TSS63/TSS	TSS63 Total Load B_{TSS63}	TSS63 Removal Efficiency $\eta_{B,63}$	TSScoarse Total Load $B_{TSScoarse}$	TSScoarse Removal Efficiency $\eta_{B,coarse}$
-	-	kg	-	kg	%	kg	%
SG	Inflow	1413	0.78	1102	19	242	59
	Outflow	1006	0.89	895		98	
CG	Inflow	556	0.79	439	16	92	28
	Outflow	452	0.82	370		66	

Figure 5a for site SG and Figure 5b for site CG show the event-specific relationship between inflow and outflow loads. The additional boxplots for inflow and outflow loads summarize the statistical description of all events and show the mean, median, 0.25 and 0.75 percentile, whiskers for 1.5 IQR, and max values.

Values under the separation line indicate a positive removal efficiency, whereas values above the line indicate a negative efficiency. At site SG, events with negative efficiencies are visible, which occurred in period 2 and therefore have a decreasing effect on the removal efficiency in comparison to period 1. At site CG, events with negative efficiencies occurred in periods 1 and 2. Removal efficiency ranged between −120% and 100% at site SG, and −35% to 96% at site CG. TSS load mean values decreased at each site from inflow to outflow, from 16.4 to 11.2 kg at site SG, and 13.9 to 11.0 kg at site CG.

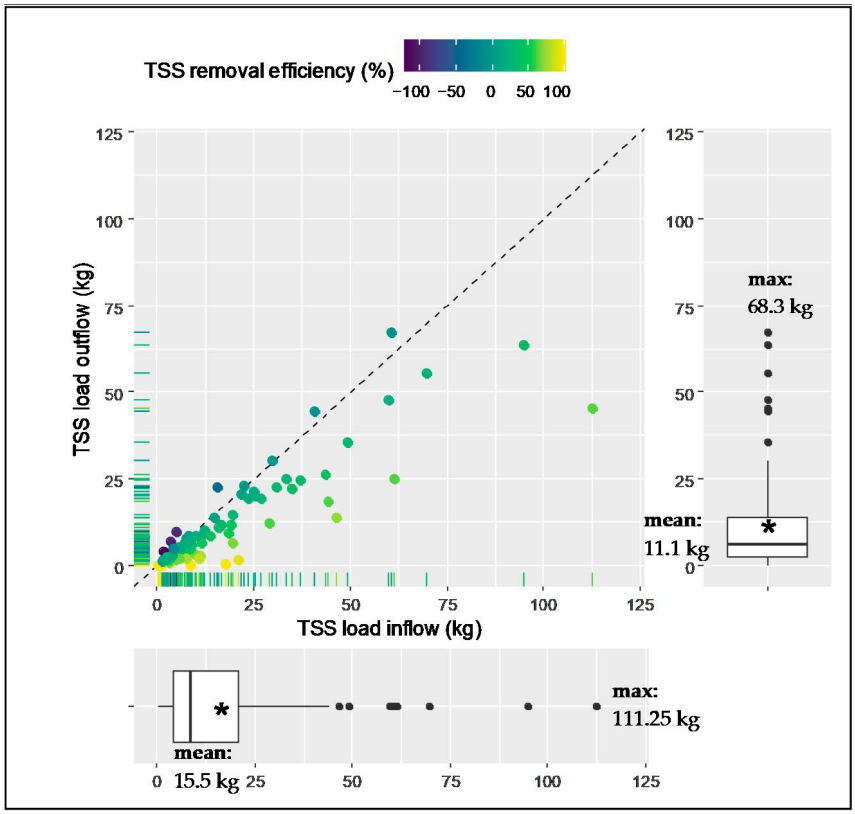

(a) site SG

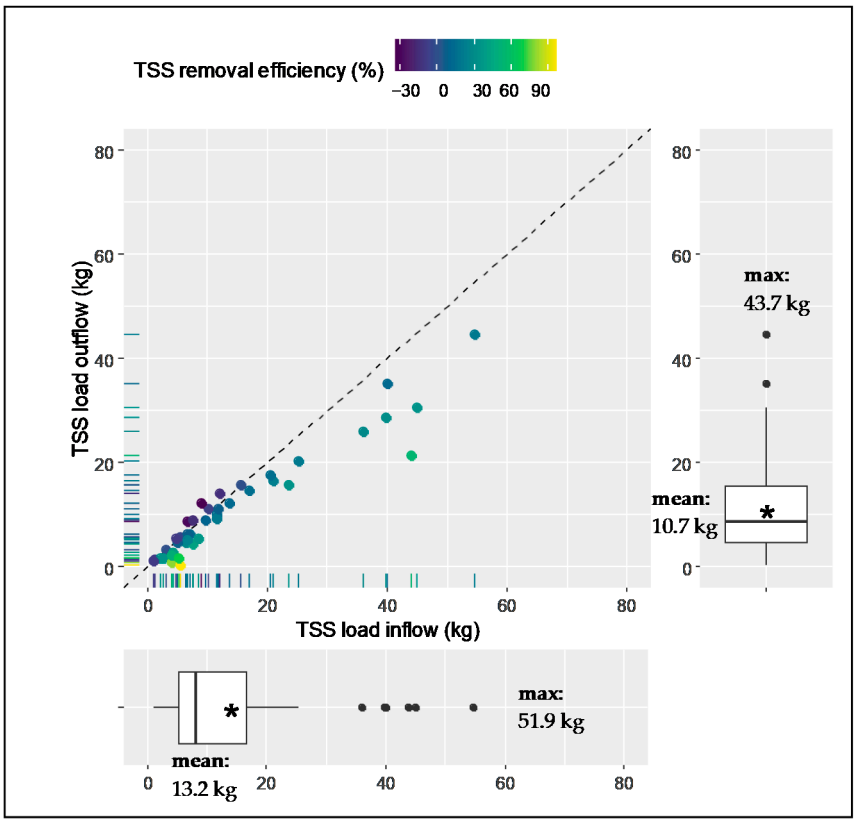

(b) site CG

Figure 5. Event-specific TSS loads of in- and outflows with event-specific TSS removal efficiency at the sites SG (**a**) and CG (**b**); "*" = mean values in boxplots; figure modified from [46]. Outliers are indicated as black dots.

By applying the rain event selection criteria (H > 2 mm and Imax60 > 2 mm/h) on the monitored rain sum (2126 mm) the effective rain sum was determined (1653 mm). For each site, the event rain sum per year was divided by the effective rain sum per year.

The resulting rain treatment ratios are listed together with the seasonal event distribution in Table 6. The highest value per year and total treatment ratio were at site SG, with values of 0.61 (2018) and 0.49 (total). Due to a later monitoring start in 2018 and fewer events in 2020, the treatment ratios for DS2 at site CG were lower, with the highest being 0.36 (2019) and a total of 0.27. At both sites, the seasonal event distribution showed fewer events in spring. Most events were recorded in winter and fall at site SG. At site CG most events were recorded in fall and summer.

Table 6. Precipitation representativity and seasonal distribution of events at site SG and CG.

Year	Rain Sum	Effective Rain Sum	Site SG		Site CG	
			Treated Rain	Treatment Ratio	Treated Rain	Treatment Ratio
From - to	mm	mm	mm	-	mm	-
November 2017->	189	137	69.0	0.51	-	-
2018	578	403	246	0.61	71.9	0.27 [1]
2019	762	630	226	0.36	224	0.36
->December 2020	597	483	266	0.55	71.6	0.15 [2]
Total	2126	1653	806	0.49	387	0.27 [1]
Events per Season	SG (n = 91) Spring n = 18 Summer n = 21 Fall n = 24 Winter n = 28 CG (n = 51) Spring n = 7 Summer n = 15 Fall n = 16 Winter n = 13					

[1] 05/2018 = beginning of monitoring at site CG, with lower rain sum of 268 mm for ratio calculation, [2] system all year in operation but sensor failure.

3.4. Uncertainty of TSS Load Removal Efficency

After data processing, the relative residuals Δc^* were analyzed for in- and outflow of both DS. The standard deviations given in Table 7 were used as estimates for the uncertainties $u_c^* = s_{\Delta c^*}$ per sample position.

Table 7. Standard deviation and mean values for relative residuals per site and sample position.

	Relative Residuals Δc^*			
	SG Inflow	SG Outflow	CG Inflow	CG Outflow
n	182	83	181	166
Mean	0.000904	0.00711	0.261	0.0774
$s_{\Delta c^*}$	0.824	0.554	1.03	1.80

The uncertainty u_η of the removal efficiency for two selected runoff events at both sites in Table 8 show low values at site SG and moderate to large values at site CG. This corresponds to the standard deviations of the relative residuals Δc^*. Because the removal efficiencies η are low in all cases the relative uncertainties u_η^* are high and extremly high for event CG-109 with a very low removal efficiency.

Table 8. Uncertainties for selected events at SG and CG.

Event	$\Sigma\dot{m}_{E,in}$	$\Sigma\dot{m}_{E,out}$	$\Sigma u_{B,E,in}$	$\Sigma u_{B,E,out}$	$\eta\,\frac{\Sigma_{B,E,out}}{\Sigma_{B,E,in}}$	$u\,\frac{\Sigma_{B,out}}{\Sigma_{B,in}}$	u_η	u_η^*	Duration
site-ID	g/s	g/s	-	-	%	%	%	%	hh:mm
SG-1	59.3	46.6	3.17	1.71	21.0	5	5	24	04:26
SG-159	261	192	8.81	4.24	26.4	3	3	11.3	08:01
CG-15	41.2	28.3	2.77	3.35	31	9	9	30	07:55
CG-109	80.3	76.0	11.0	11.0	5	19	19	353	11:35

3.5. Mass Balance

A calculation of mass balance was conducted due to time proportional sampling and constantly pumped discharge at the site SG. The calculation is based on TSS concentration

samples for the first two hours of an event. Only data pairs of in- and outflow concentrations were used. Table 9 lists the results of the mass balance for 75 sample pairs out of nine events. The DS1 achieved a removal efficiency of 47% during the sampling time frame of 2 h. The TSS63 ratios per sample were summarized for inflow and outflow to note the TSS63 shift of 5.3% due to treatment.

Table 9. Mass balance, TSS load removal efficiency and TSS63 sum for composite sample pairs at site SG.

Events	Sample Pairs	Q Sampled	B_{in}	B_{out}	Removal Efficienc η_B	TSS63 Ratio Sum In	TSS63 Ratio Sum Out	TSS63 Ratio Shift
-	-	m^3	kg	kg	%	-	-	%
9	75	270	63.0	33.5	47	63.3	66.7	5.3

4. Discussion

4.1. Relation between TSS and Turbidity

For long-term monitoring, a consistent TSS63 ratio is crucial to obtain a sufficient conversion of turbidity to TSS. One key factor is the correct installation of turbidity-sensors at the in- and outflow of a DS. DS of smaller size might lack enough space for installation, which is crucial to ensure correct turbidity measurements without signal interference from DS walls or tubes.

For all sample positions, reliable regression coefficients were determined. The TSS analysis at both sites showed intra-event runoff with variable TSS concentrations but with consistent high proportions of TSS63 (cf. Appendix A Table A2) in the range of 0.78 to 0.89 in average. During data preparation, samples with TSS63 ratio < 0.5 and high leverage were excluded for linear regression. Selection of samples with higher TSS63 ratio for regression of turbidity to TSS can lead to a lower slope, whereas exclusion of high leverage samples can have an effect in both directions. A lower slope for conversion of turbidity data to TSS would lead to a lower load in total at the specific sample position, which contributes direct to the long-term removal efficiency. Slope decreased only for SG inflow from 1.21 to 0.96. At site CG, slope increased from 0.84 to 0.91 (inflow) and 0.94 to 0.99 (outflow). Values of regression were comparable for slope in the range of 0.91 to 0.99. Against this background, a higher influence of the turbidity on the slope due to a higher TSS63 ratio at the respective DS outflows was expected but could not be confirmed by the coefficients. The intercept deviated from 2.31 (in) to −0.41 (out) at SG and from −1.94 (in) to −3.96 (out) at CG. Because these values are negative, an effect with changed boundary conditions (0/0) on slope and final uncertainties must be investigated further.

For the linear regression of SG inflow a comparison to previous sewer data (2015, n = 85) of the identical extraction point is available. The linear regressions differ only in intercept, with values of 7.93 (2015) and 2.31 (2018–2019). The previous data's slope b = 0.97 is comparable to the current b = 0.99. The coefficients of determination are equal, with R^2 = 0.68 (2015) and R^2 (adjusted) = 0.75 (2018–2019). This indicates a similar site-specific TSS matrix over the long-term.

The total number of used samples per regression ranged from 83 to 182. The magnitude of the difference between raw data samples and prepared data samples was the lowest at 8 (SG, outflow) and the highest at 40 (CG, inflow). The relative sample reduction during data processing was 9% to 18%, with an average of 13%. After data processing, the R^2 (adjusted) was higher by 0.33 on average, except for SG outflow that remained the same with R^2 (adjusted) of 0.75. The chosen statistical criteria to ensure a better fit of linear regression over the long-term cam be recommended. Due to the reliable fit of the individual regressions per sample position, the parameter turbidity can be used as a surrogate for TSS to monitor long-term removal efficiency of DS.

4.2. TSS Load Removal Efficencies and Uncertainties

The analysis of TSS load removal for DS1 showed a long-term efficiency of $\eta_{B,TSS}$ = 40% in period 1 (n = 51 events) and $\eta_{B,TSS}$ = 29% (n = 91 events) over the full monitoring cycle.Further removal efficiency estimations for TSS63 and TSScoarse are $\eta_{B,TSS63}$ = 16% and $\eta_{B,TSScoarse}$ = 59%. The composite sample-based mass balance for period 1 (n = 75 samples, nine events) resulted in $\eta_{B,TSS}$ = 47% for the first two event hours and effected a TSS63 ratio shift of 5.3%. A DS performance rating based on mass balance or monitoring results of period 1 would overestimate the long-term efficiency, because 2018 was a dry year with the highest observed TSS concentrations in urban stormwater runoff. Therefore, the result of period 2 (2018–2020) allowed a better assessment. Uncertainty evaluation of selective events at SG showed variable u_η of 3% to 5% with relative uncertainty u_η^* of 9% to 30%. Further evaluation is necessary to achieve reliable uncertainties according to long-term removal efficiency. The estimated higher removal efficiency for TSScoarse particles displayed a theoretical in situ performance peak of the DS, when influent contained no particles < 63 µm. However, the lower removal efficiency for fine particles indicates an achievable value in the case of a high TSS63 ratio. Due to variance in the ratio of TSS63 to TSS and seasonal difference in temperature, organic pollution compartments, and therefore, particle density and potential to aggregate to conglomerates, additional factors have an influence on removal efficiency if reduction is only targeted by sedimentation [47]. For example, no remobilization or outwash was recorded in the first period at DS1, but in period 2. Visual analysis of such an event with a negative efficiency in fall showed a high rest turbidity in the outflow from the previous event (criteria to separate events = rain stop > 4 h). One assumption is, that the high rest turbidity occurred due to a high ratio and concentration of TSS63 combined with a low density of particles. Remobilization due to varying hydraulic inflow can be excluded due to constant pump inflow of 6 L/s. Investigations of environmental conditions and DS settings of these event phenomena would be informative. To obtain more clarity of event concentration even after monitoring implementation, a time-integrated full event composite sample backup would be beneficial. Furthermore, the DS1 was inspected and cleaned in July 2019 and October 2020 according to the maintenance instructions.

At site CG, for DS2 the long-term removal efficiency was $\eta_{B,TSS}$ = 19%, whereas for TSS63 and TSScoarse they were $\eta_{B,TSS63}$ = 16% and $\eta_{B,TSScoarse}$ = 28%, respectively. The DS2 TSS removal efficiency for periods 1 and 2 remained the same. This constant long-term efficiency could represent a consistent treatment. Nonetheless, the lack of difference was because fewer new events in period 2 were monitored. Additionally, the events in period 2 had a lower runoff pollution of TSS and, therefore, had a lower leverage on the overall removal efficiency. Uncertainty evaluation of selective events at CG showed high variable u_η of 9% to 19% with high and extremely high relative uncertainty u_η^* of 30% to 353%. The monitoring of DS2 resulted in a low long-term efficiency with high uncertainties. One variable that has contributed to the low efficiency is the low TSS concentration. The median inflow TSS concentration of 25.4 mg/L was close to minimum TSS concentration of 20 mg/L from [19] to be considered as an assessable pollution event. In addition, the DS2 manufacturer declares a separation only for particles with a size range down to 0.1 mm [48]. Therefore, the DS2 is not applicable for urban stormwater runoff treatment with such a high TSS63 ratio. The observed removal efficiencies were only conclusive for the configured throttle discharge of max 35 L/s. Negative removal efficiencies might be caused by high proportions of fine particle material or too high flow rates. Under these site-specific conditions, the DS operator should check the throttle function and examine the option of throttle reduction to improve DS performance.

In addition to the focused TSS removal of particles with a maximum size of 2 mm, DS2 removed more granular particles with its lamella clarifier. During maintenance observation in November 2020, mud levels up to 60 and 30 cm were observed at the in- and outflow chambers, respectively. The high mud level in the outflow chamber amplifies the theory of strong remobilization due to high discharges that were able to transport even coarse

material through and over the lamella clarifier to the outflow chamber and from there to the river. The mud consisted mostly of sand, leaves, sticks, and cigarette butts. The exact composition of the mud must be analyzed further.

4.3. TSS and TSS63 in Urban Stormwater Runoff

In both monitored DS, the stormwater runoff is primarily treated by sedimentation of particles. The effectiveness was tested and demonstrated for both DS according to the lab based test [21] with the inorganic TSS-surrogate quartz flour "Milli Sil W4". Therefore, first, a TSS concentration reduction in terms of lower mean and median values, and, second, a change in the particle size distribution, were expected from inflow to outflow, because coarser particles tend to sediment rather than finer particles.

A TSS reduction between inflow and outflow can be recognized for DS1 by lower mean, median, and sd values. For DS2, the mean and sd values were lower in the inflow than in the outflow. However, the median value was higher in the inflow than in the outflow as expected. The inequality of mean values in composite samples could occur from a low TSS concentration combined with remobilization, which might have been covered due to sampling. The previously recorded TSS concentration values of the sewer at site SG in 2015 are lower than our recorded values. A loss of TSS due to pumping can therefore be discounted.

The mean TSS63 ratios were similar in the inflow at both sites (0.78 SG and 0.79 CG). Other studies report equal TSS63 ratios for road runoff, with values of 0.82 and 0.85 [12,16]. After treatment, the ratios shifted differently. At SG, the mean TSS63 ratio in the outflow increased to 0.89, which was reported as a significant difference by ANOVA. This shift indicates a more effective reduction of TSScoarse with particle size > 63 µm. At CG, the increased outflow TSS63 ratio mean of 0.82 was smaller and the difference is not significant.

The urban stormwater runoff pollution differed in concentration between sites. Because wash off processes were not considered in this study, no detailed statements can be made, except that the daily average vehicle and cover of the impervious area were higher at SG than at CG. Selbig 2015 [16] shows with a particle size distribution (PSD) of urban stormwater runoff a median particle diameter (d_{50}) of 8, 32, 43, 50, 80, and 95 µm for six different types of land use, with a collector street yielding the lowest d_{50}. As an outcome, it must be assumed that TSS63 contributes with a minimum of 50% to the urban stormwater runoff pollution and even higher for streets.

4.4. Indications for Further Planning and Operation of DS

Urban stormwater runoff consists of high proportions of TSS63, which can significantly affect the ecological quality of receiving waters. During rain events with a high stormwater runoff concentration of TSS, as recorded in 2018, increased removal efficiencies were observed. Before installation of a new DS, the pollution characteristics of catchments should be evaluated, for the concentrations and ratios of TSS63 and TSScoarse over several events. It must be considered whether an exclusive sediment treatment is sufficient for TSS loads with high TSScoarse ratio or if filtration is more suitable according to a dominant TSS63 ratio.

Sansalone (1997) shows that heavy metals, such as Zn, Cd, and Cu, are mainly dissolved and their proportion of the total concentration underlies seasonal influences [11]. This observation indicates that a filtering technique should be considered in the design of DS if treatment of high polluted urban stormwater runoff is targeted. Manufacturers already invented exchangeable filter-cassettes targeting this demand.

4.5. Improvement of DS Evaluation

Results from the lab and in situ tests differed. The treatment and removal of fine particles should be the main objective of DS. This could be tested simply in a laboratory by implementation of two further tests. The tests could be conducted by manufactured predefined critical discharge and two fractions of TSS surrogate with (a) particles only

>63 µm and (b) with particles only <63 µm. This would show the range of possible removal efficiency values for the TSS shares.

To improve and validate our in situ monitoring approach, it would be beneficial to validate the turbidity measurements of in- and outflow during lab test. As an outcome, this could provide a further standard for the installation of sensors at a DS. Obligatory turbidity measurements during laboratory tests would greatly facilitate and deepen the process analysis of the in situ data.

In situ investigations of DS are regarded to be mandatory for performance assessments due to the highly variable processes of pollutant build-up, wash-off, and transport processes of storm water runoff in terms of time and place.

5. Conclusions

Two different decentralized stormwater treatment systems (DS) at two different sites were monitored for 2 to 3 years. Continuous turbidity data and composite samples from inflow and outflow were used to evaluate the in situ TSS and TSS63 removal efficiency. From the analysis it can be concluded that:

- In situ treatment is not at par with lab results. Even with constant hydraulic conditions, high variability of efficiency was observed.
- For the two monitored sites with a high mean TSS63 ratio of 0.8, sedimentation treatment does not meet the treatment objective to adequately protect the receiving water and exposed organisms.
- The significant TSS63 ratio shift from inflow to outflow indicated that DS with an exclusive sedimentation treatment can achieve better removal efficiencies with respect to coarser particles (>63 µm).
- The TSS63 as a new stormwater design parameter and especially its fraction of TSS should be given more attention to characterize stormwater quality as it affects the correlation to turbidity.
- It is well known that using turbidity as a proxy of TSS introduces uncertainties. However, as the explorative results indicated, further investigations especially when evaluating the removal efficiency of DS are strongly recommended.
- Due to the physics of sedimentation and its limits, treatment of urban stormwater runoff with high TSS63 pollution requires additional techniques, such as filtering to retain fine particles more effective.

Decentralized stormwater treatment systems are complementing measures for efficient stormwater management. With the introduced online-monitoring concept in situ insights of the performance were gained.

Author Contributions: C.L.: paper coordination and writing, data analysis, visualization. D.L.: project concept and funding, methodology, data management and analysis, supervision, and contributions. M.U.: project concept and funding, uncertainty analysis, supervision, and contributions. All authors have read and agreed to the published version of the manuscript.

Funding: The research work and software developments are part of the research project "Leistungsfähigkeit großer dezentraler Niederschlagswasserbehandlungsanlagen unter realen Betriebsbedingungen" (DezNWBA Phase 1 and Phase 2) which has been supported by the Ministry for Environment, Agriculture, Conservation and Consumer Protection of the State of North Rhine-Westphalia (MULNV NRW).

Institutional Review Board Statement: Not applicable.

Informed Consent Statement: Not applicable.

Data Availability Statement: Restrictions apply to the availability of these data. Data was obtained for MULNV NRW and are available from the authors with the permission of MULNV NRW. Sampling data is contained within the article Appendix A.

Acknowledgments: The project "DezNWBA" was funded by the Ministry for Environment, Agriculture, Conservation and Consumer Protection of the State of North Rhine-Westphalia (MULNV NRW). The authors would like to thank the staff of MULNV NRW for their professional support and the City of Münster for their support and cooperation at the monitoring sites.

Conflicts of Interest: The authors declare no conflict of interest.

Appendix A

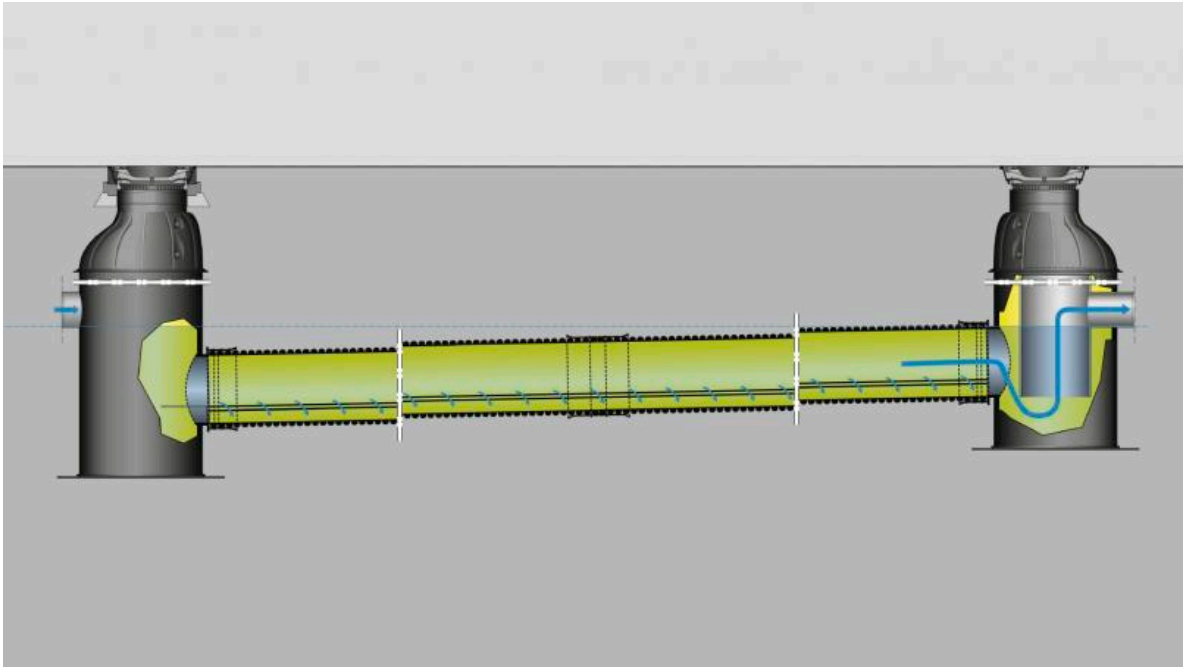

(**a**)

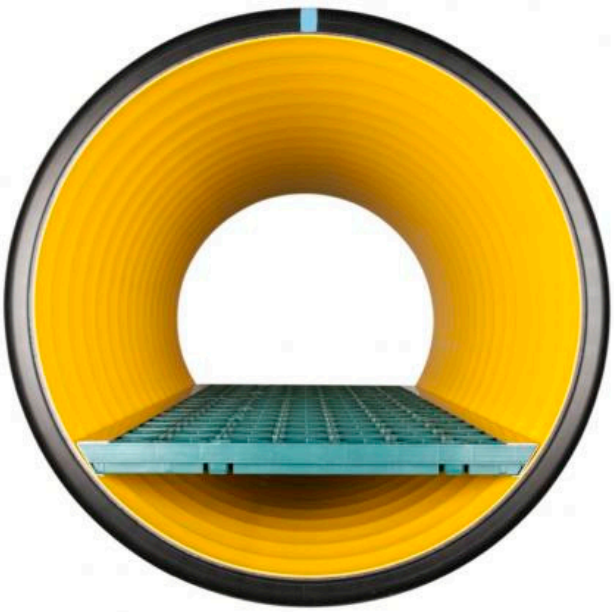

(**b**)

Figure A1. Schematic of the SediPipe XL 600/12 in lateral section (**a**) and in cross section (**b**) [49].

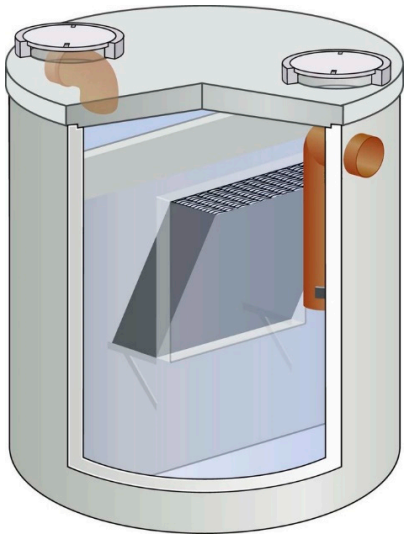

(**a**)

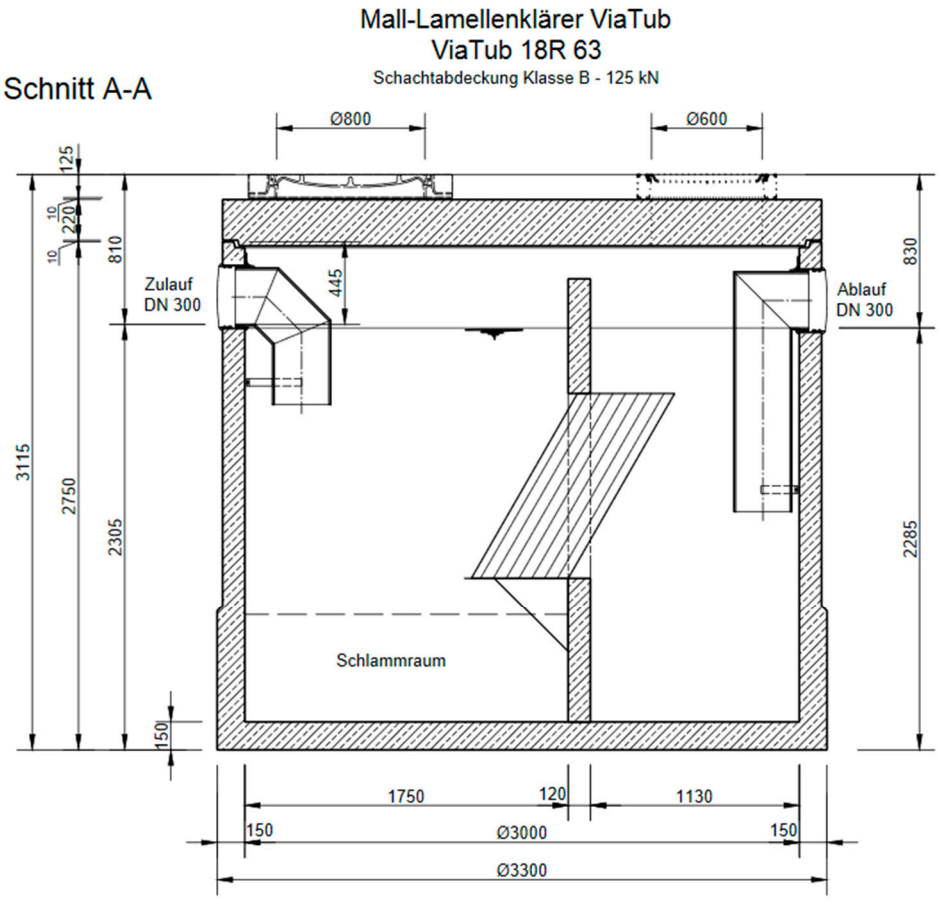

(**b**)

Figure A2. Illustration (**a**) and technical schematic (**b**) of the lamella clarifier (DS2) [48].

Table A1. Rain statistic for events covered by automatic sampling.

		Rain Event			
Site	**Date**	**Duration**	**Sum**	**Mean**	**Imax60**
-	**-**	**h**	**mm**	**mm**	**mm/h**
Canisiusgraben	10 May 2018	6.7	3.1	0.5	1.4
	29 August 2018	9.9	11.9	1.2	5.3
	30 August 2018	9.9	11.9	1.2	5.3
	6 September 2018	2.8	5.0	1.8	3.4
	21 September 2018	0.8	3.8	4.9	4.9
	06 October 2018	0.4	0.4	3.6	1.0
	24 October 2018	29.7	7.6	0.3	1.2
	26 October 2018	2.6	3.5	1.3	3.0
	10 November 2018	1.2	1.0	0.8	0.9
	14 November 2018	0.0	0.1	1.5	1.5
	20 November 2018	3.0	1.9	0.6	1.4
	28 November 2018	2.4	0.8	0.3	0.5
	4 December 2018	5.2	3.1	11.4	0.6
	17 December 2018	10.6	2.0	0.2	0.4
	6 January 2019	35.9	8.1	0.2	1.1
	1 February 2019	2.6	1.7	0.7	1.2
	4 February 2019	0.0	0.1	2.4	2.4
	10 February 2019	20.4	22.0	12.6	1.1
	24 April 2019	0.3	1.9	19.2	7.2
	26 April 2019	3.0	1.5	0.5	1.3
	2 May 2019	1.9	0.5	0.3	0.3
	3 May 2019	2.8	1.5	6.6	0.6
	19 May 2019	1.6	0.8	0.5	0.5
	21 May 2019	0.6	0.4	0.7	0.7
	6 July 2019	4.1	4.9	1.2	2.7
Stadtgraben	1 January 2018	2.3	5.3	2.3	3.4
	31 January 2018	15.4	13.6	0.9	5.0
	8 March 2018	5.5	8.1	1.5	4.2
	10 March 2018	7.3	4.4	0.6	1.0
	13 March 2018	5.5	1.3	0.2	0.5
	23 March 2018	2.5	0.2	0.1	0.1
	28 March 2018	7.9	14.1	1.8	4.0
	26 April 2018	2.6	1.8	0.7	1.7
	28 July 2018	0.6	2.8	5.0	5.0
	8 August 2018	2.3	0.3	5.4	0.13
	20 December 2018	11.3	5.9	0.5	2.9
	10 January 2019	10.4	2.7	3.6	0.26
	17 January 2019	13.8	5.4	0.4	2.2
	28 January 2019	17.8	9.0	0.5	5.0
	1 February 2019	2.6	1.7	0.7	1.2
	1 March 2019	5.1	1.7	0.3	1.1
	6 March 2019	0.8	1.3	1.6	1.6
	24 April 2019	0.3	1.9	7.2	7.2
	6 June 2019	3.4	4.2	1.2	3.1

Table A2. Descriptive statistics of TSS concentration, TSS63-ratio, and turbidity from bottle samples per site and sample position, with TSS values in mg/L and turbidity in FNU. Samples were taken from January 2018 until July 2019.

Site	Sample Position	Parameter	n	TSS Concentration (mg/L)										
				Mean	Sd	0%	5%	10%	25%	50%	75%	90%	95%	100%
SG	Inflow	TSS63/TSS	210	0.78	0.19	0.051	0.37	0.53	0.69	0.84	0.93	0.96	0.98	1
		TSS63	210	94.4	101	2.84	8.82	12.2	18.6	62.6	134	229	328	513
		TSS	210	27.1	168	5.21	13.5	14.7	27.0	81.2	155	276	381	1398
		TSS in Turb	210	97.9	127	4.03	10.4	11.2	20.1	63.2	121	220	296	938
		Turbidity	210	84.2	69.7	5.70	11.8	15.0	26.1	69.5	126	181	226	306
	Outflow	TSS63/TSS	91	0.89	0.17	0.034	0.61	0.74	0.89	0.94	0.98	0.99	0.99	1
		TSS63	91	97.9	86.1	0.68	4.92	12.0	26.6	67.6	162	235	260	315
		TSS	91	03.3	86.8	1.07	13.9	17.8	31.6	69.2	171	241	269	324
		TSS in Turb	91	82.0	70.6	0.81	11.2	13.4	25.3	57.8	119	201	220	250
		Turbidity	91	88.1	63.7	1.50	14.2	18.0	40.0	71.0	130	185	220	246
CG	Inflow	TSS63/TSS	221	0.79	0.19	0.05	0.46	0.51	0.67	0.87	0.93	0.97	0.98	1
		TSS63	221	31.0	43.6	0.55	2.40	4.58	9.81	19.6	37.1	65.6	76.1	410
		TSS	221	38.4	49.7	1.55	3.60	7.57	13.5	25.4	47.0	74.9	104	432
		TSS in Turb	221	29.9	39.7	1.25	2.88	5.73	10.5	19.3	35.4	58.1	77.2	356
		Turbidity	221	36.8	38.4	2.50	4.50	7.00	12.0	25.7	48.0	73.0	102	295
	Outflow	TSS63/TSS	189	0.82	0.19	0.0055	0.46	0.61	0.76	0.88	0.95	0.98	0.99	1
		TSS63	189	34.2	56.3	0.36	1.48	2.17	5.15	16.8	39.2	74.7	98.2	456
		TSS	189	46.0	81.4	1.06	2.02	2.96	7.90	21.2	46.4	89.8	179	579
		TSS in Turb	189	37.8	68.8	0.89	1.69	2.48	5.95	17.0	39.0	75.9	136	498
		Turbidity	189	36.9	49.0	2.20	3.48	4.28	7.20	20.1	44.0	94.0	113	345

References

1. Ellis, J.; Hvitved-Jacobsen, T. Urban drainage impacts on receiving waters. *J. Hydraul. Res.* **1996**, *34*, 771–783. [CrossRef]
2. Walsh, C.J.; Fletcher, T.D.; Burns, M.J. Urban Stormwater Runoff: A New Class of Environmental Flow Problem. *PLoS ONE* **2012**, *7*, e45814. [CrossRef] [PubMed]
3. Yang, Y.-Y.; Lusk, M.G. Nutrients in Urban Stormwater Runoff: Current State of the Science and Potential Mitigation Options. *Curr. Pollut. Rep.* **2018**, *4*, 112–127. [CrossRef]
4. Chebbo, G.; Gromaire, M.; Ahyerre, M.; Garnaud, S. Production and transport of urban wet weather pollution in combined sewer systems: The "Marais" experimental urban catchment in Paris. *Urban Water* **2001**, *3*, 3–15. [CrossRef]
5. Göbel, P.; Dierkes, C.; Coldewey, W. Storm water runoff concentration matrix for urban areas. *J. Contam. Hydrol.* **2007**, *91*, 26–42. [CrossRef] [PubMed]
6. Becouze-Lareure, C.; Dembélé, A.; Coquery, M.; Cren-Olivé, C.; Barillon, B.; Bertrand-Krajewski, J.-L. Source characterisation and loads of metals and pesticides in urban wet weather discharges. *Urban Water J.* **2016**, *13*, 600–617. [CrossRef]
7. Ellis, J.; Revitt, D.; Harrop, D.; Beckwith, P. The contribution of highway surfaces to urban stormwater sediments and metal loadings. *Sci. Total Environ.* **1987**, *59*, 339–349. [CrossRef]
8. Launay, M.A.; Dittmer, U.; Steinmetz, H. Organic micropollutants discharged by combined sewer overflows—Characterisation of pollutant sources and stormwater-related processes. *Water Res.* **2016**, *104*, 82–92. [CrossRef] [PubMed]
9. Zgheib, S.; Moilleron, R.; Chebbo, G. Priority pollutants in urban stormwater: Part 1—Case of separate storm sewers. *Water Res.* **2012**, *46*, 6683–6692. [CrossRef]
10. Aryal, R.; Vigneswaran, S.; Kandasamy, J.; Naidu, R.; Vigneswaran, S. Urban stormwater quality and treatment. *Korean J. Chem. Eng.* **2010**, *27*, 1343–1359. [CrossRef]
11. Sansalone, J.J.; Buchberger, S.G. Characterization of Solid and Metal Element Distributions in Urban Highway Stormwater. *Water Sci. Technol.* **1997**, *36*, 155–160. [CrossRef]
12. Hilliges, R.; Endres, M.; Tiffert, A.; Brenner, E.; Marks, T. Characterization of road runoff with regard to seasonal variations, particle size distribution and the correlation of fine particles and pollutants. *Water Sci. Technol.* **2017**, *75*, 1169–1176. [CrossRef]
13. DWA-A 102-1. *Grundsätze zur Bewirtschaftung und Behandlung von Regenwasserabflüssen zur Einleitung in Oberflächengewässer—Teil 1: Allgemeines*; Deutsche Vereinigung für Wasserwirtschaft, Abwasser und Abfall e. V. (DWA): Hennef, Germany, 2020; ISBN 978-3-96862-044-2.
14. Dierschke, M.; Welker, A. Bestimmung von Feststoffen in Niederschlagsabflüssen. *GWF Wasser Abwasser* **2015**, *156*, 440–446.
15. Zhao, H.; Li, X.; Wang, X.; Tian, D. Grain size distribution of road-deposited sediment and its contribution to heavy metal pollution in urban runoff in Beijing, China. *J. Hazard. Mater.* **2010**, *183*, 203–210. [CrossRef] [PubMed]
16. Selbig, W.R. Characterizing the distribution of particles in urban stormwater: Advancements through improved sampling technology. *Urban Water J.* **2013**, *12*, 111–119. [CrossRef]
17. Sommer, H.; Post, M.; Estupinan, F.; Ingenieurgesellschaft Prof. D. Sieker mbH. *Dezentrale Behandlung von Straßenabflüssen—Übersicht Verfügbarer Anlagen*. 2016. Available online: https://www.sieker.de/fileadmin/sieker/Buero/veroeffentlichungen/Broschuere_Dezentrale_Regenwasserbehandlung_2016.pdf (accessed on 25 March 2021).
18. Geosyntec Consultants; Wright Water Engineers, Inc. *Urban Stormwater BMP Performance Monitoring*; US Environmental Protection Agency: Washington, DC, USA, 2009.
19. Department of Ecology State of Washington. Technical Guidance Manual for Evaluating Emerging Stormwater Treatment Technologies. Technology Assessment Protocol—Ecology (TAPE). Available online: https://ecology.wa.gov/Regulations-Permits/Guidance-technical-assistance/Stormwater-permittee-guidance-resources/Emerging-stormwater-treatment-technologies (accessed on 13 December 2020).
20. VSA-Leistungsprüfung für Behandlungsanlagen, Merkblatt «Leistungsprüfung für Adsorbermaterialien und Dezentrale Technische Anlagen zur Behandlung von Niederschlagswasser». Available online: https://vsa.ch/Mediathek/vsa-leistungspruefung-fuer-behandlungsanlagen/ (accessed on 11 February 2021).
21. DIBt (Deutsches Institut für Bautechnik). *Zulassungsgrundsätze für Niederschlagswasserbehandlungsanlagen*; Teil 1: Anlagen zur dezentralen Behandlung des Abwassers von Kfz-Verkehrsflächen zur anschließenden Versickerung in Boden und Grundwasser; DIBt (Deutsches Institut für Bautechnik): Berlin, Germany, 2015.
22. Lucke, T.; Nichols, P.; Shaver, E.; Lenhart, J.; Welker, A.; Huber, M. Pathways for the Evaluation of Stormwater Quality Improvement Devices—The Experience of Six Countries. *CLEAN Soil Air Water* **2017**, *45*, 1600596. [CrossRef]
23. Leutnant, D.; Muschalla, D.; Uhl, M. Stormwater Pollutant Process Analysis with Long-Term Online Monitoring Data at Micro-Scale Sites. *Water* **2016**, *8*, 299. [CrossRef]
24. Gruber, G.; Winkler, S.; Pressl, A. Quantification of pollution loads from CSOs into surface water bodies by means of online techniques. *Water Sci. Technol.* **2004**, *50*, 73–80. [CrossRef]
25. Bertrand-Krajewski, J.-L. TSS concentration in sewers estimated from turbidity measurements by means of linear regression accounting for uncertainties in both variables. *Water Sci. Technol.* **2004**, *50*, 81–88. [CrossRef]

26. Caradot, N.; Sonnenberg, H.; Rouault, P.; Gruber, G.; Hofer, T.; Torres, A.; Pesci, M.; Bertrand-Krajewski, J.-L. Influence of local calibration on the quality of online wet weather discharge monitoring: Feedback from five international case studies. *Water Sci. Technol.* **2014**, *71*, 45–51. [CrossRef]
27. Métadier, M.; Bertrand-Krajewski, J.-L. The use of long-term on-line turbidity measurements for the calculation of urban stormwater pollutant concentrations, loads, pollutographs and intra-event fluxes. *Water Res.* **2012**, *46*, 6836–6856. [CrossRef] [PubMed]
28. Bertrand-Krajewski, J.-L.; Chebbo, G.; Saget, A. Agnes Distribution of Pollutant Mass vs. Volumen in Stormwater Discharges and the First Flush Phenomen. *Water Res.* **1998**, *32*, 2341–2356. [CrossRef]
29. Bertrand-Krajewski, J.-L. Stormwater pollutant loads modelling: Epistemological aspects and case studies on the influence of field data sets on calibration and verification. *Water Sci. Technol.* **2007**, *55*, 1–17. [CrossRef] [PubMed]
30. Uhl, M.; Mohn, R.; Maus, C.; Schnieders, A.; Sommer, M.; Voßwinkel, N.; Ebbert, S.; Tenbeitel, J.-G. *Weitergende Regenwasserbehandlung Im Trennsystem (WEREBE)*; FH Münster Institut für Wasser·Ressourcen·Umwelt (IWARU): Münster, Germany, 2013.
31. WTW GmbH. *Operating Manual VisoTurb 700 IQ (SW)*. 2017. Available online: https://www.xylemanalytics.com/en/File%20Library/Resource%20Library/WTW/01%20Manuals/ba57301e09_VisoTurb_700_IQ_SW_WTW.pdf (accessed on 25 March 2020).
32. Nivus GmbH. *Technical Instructions for Correlation Sensors and External Electronic Box*. 2019. Available online: http://www.nivus.de/ximages/1404786_sasba02en.pdf (accessed on 11 February 2021).
33. OTT Hydromet GmbH. *Betriebsanleitung Niederschlagssensor OTT Pluvio^2 L*. 2013. Available online: https://www.lufft.com/de-de/produkte/download-de/betriebsanleitung-ott-pluvio2-l-de/ (accessed on 25 March 2021).
34. DIN 38409-2. *Summarische Wirkungs—Und Stoffkenngrößen (Gruppe H)—Bestimmung Der Abfiltrierbaren Stoffe Und Des Glührückstandes (H 2)*; Beuth Verlag GmbH: Berlin, Germany, 1987.
35. NEMI Method Summary-160.2—Residue. Non-Filterable (Gravimetric. Dried at 103–105 °C). Available online: https://www.nemi.gov/methods/method_summary/5213/ (accessed on 13 December 2020).
36. 2540 Solids. Available online: https://www.standardmethods.org/doi/ref/10.2105/SMWW.2882.030 (accessed on 13 December 2020).
37. Baum, P.; Benisch, J.; Blumensaat, F.; Dierschke, M.; Dittmer, U.; Gelhardt, L.; Gruber, G.; Grüner, S.; Heinz, E.; Hofer, T.; et al. AFS63—Harmonisierungsbedarf Und Empfehlungen Für Die Labortechnische Bestimmung Des Neuen Parameters. In Proceedings of the Regenwasser in urbanen Räumen—Aqua urbanica trifft RegenwasserTage 2018, Landau in der Pfalz, Germany, 18–19 June 2018; Schmitt, T.G., Ed.; Technische Universität Kaiserslautern: Landau in der Pfalz, Germany, 2018; Volume 1.
38. Leutnant, D.; Henrichs, M.; Muschalla, D.; Uhl, M. OSCAR—An Online Supervisory Control and Urban Drainage Data Acquisition System with R. In Proceedings of the 10th International Conference on Urban Drainage Modelling, Mont-Sainte-Anne, QC, Canada, 20–23 September 2015; Maere, T., Tik, S., Duchesne, S., Vanrolleghem, P., Eds.; pp. 135–138.
39. InfluxData. *InfluxDB*; Manual: San Francisco, CA, USA, 2020.
40. Grafana Labs. *Grafana*; Manual: New York, NY, USA; Stockholm, Sweden, 2020.
41. Leutnant, D.; Kleckers, J.; Haberkamp, J.; Uhl, M. Assessing the Performance of Decentralised Stormwater Management Measures by Means of Continuous Turbidity Measurement. In Proceedings of the Novatech 2019—10th International Conference on Urban Water—Strategies and Solutions for Sustainable Management, Lyon, France, 1–5 July 2019; p. 4.
42. R Core Team. *R: A Language and Environment for Statistical Computing*; R Foundation for Statistical Computing: Vienna, Austria, 2020.
43. Leutnant, D.; Schleifenbaum, R.; Rickert, G.; Grüning, H.; Uhl, M. *Stofftransport Und –Behandlung in Der Siedlungshydrologie (STBMOD)*; Fachhochschule Münster, Institut für Wasser·Ressourcen·Umwelt (IWARU): Münster, Germany, 2016.
44. Hannouche, A.; Chebbo, G.; Ruban, G.; Tassin, B.; Lemaire, B.J.; Joannis, C. Relationship between turbidity and total suspended solids concentration within a combined sewer system. *Water Sci. Technol.* **2011**, *64*, 2445–2452. [CrossRef]
45. JCGM 101. *Evaluation of Measurement Data—Guide to the Expression of Uncertainty in Measurement*. 2008. Available online: https://www.bipm.org/utils/common/documents/jcgm/JCGM_100_2008_E.pdf (accessed on 25 March 2021).
46. Leutnant, D.; Uhl, M. Leistungsfähigkeit Großer Dezentraler Niederschlagswasserbehandlungsanlagen Unter Realen Betriebsbedingungen. In Proceedings of the 52. ESSENER TAGUNG—Wasser in einer sich Verändernden Welt, Aachen, Germany, 20–22 March 2019; Pinnekamp, J., Ed.; Gesellschaft zur Förderung des Instituts für Siedlungswasserwirtschaft an der RWTH Aachen e. V.: Aachen, Germany, 2020.
47. Rommel, S.; Gelhardt, L.; Welker, A.; Helmreich, B. Settling of Road-Deposited Sediment: Influence of Particle Density, Shape, Low Temperatures, and Deicing Salt. *Water* **2020**, *12*, 3126. [CrossRef]
48. Mall GmbH. Lamellenklaerer ViaTub. Available online: https://www.mall.info/produkte/regenwasserbewirtschaftung/regenwasserbehandlung/viatub-lamellenklaerer/ (accessed on 9 March 2021).
49. Fränkische Rohrwerke Gebr. Kirchner GmbH & Co. KG SediPipe XL. Available online: https://www.fraenkische.com/en/product/sedipipe-xl (accessed on 9 March 2021).